

## **Effects of Ambient Pressure on R134a Sprays for Laser Dermatological Applications**

H. Vu<sup>1</sup>, W. Franco<sup>1,2</sup>, W. Jia<sup>2</sup> and G. Aguilar<sup>1,2\*</sup>

<sup>1</sup>Department of Mechanical Engineering

University of California-Riverside

Riverside, CA 92507 USA

<sup>2</sup>Beckman Laser Institute

University of California-Irvine

Irvine, CA 92617 USA

### **Abstract**

R134a sprays have been widely used as a method to protect the epidermis during laser therapies of hyper-vascular lesions, such as port wine stains, due to their high heat flux and precise control of cooling duration. Recent studies have shown that the use of vacuum cups during laser treatment can physically dilate the vasculature of interest and improve therapeutic outcome. However, the effects of these vacuum pressures, and the corresponding changes in humidity level, on the cooling sprays remain unknown. In this paper, characteristics of steady-state R134a sprays, measured with a Phase Doppler Particle Analyzer (PDPA) at different humidity levels and pressures are presented. Results show high non-uniformity in droplet characteristics across the spray cross-section at atmospheric pressures. With increasing humidity from 15 % to 75 %, no measurable changes in droplet diameter or velocity are evident, though spray cone diameter and penetration increase. Ambient pressure changes from 0 to -55 kPa, however, result in significant droplet size reductions while simultaneously increasing droplet velocities. These changes appear to occur mainly during primary atomization of the spray. The resulting implications for spray atomization and cooling effectiveness are also discussed.

---

\*Corresponding author

## Introduction

Laser treatment of various hypervascular dermatoses, particularly port wine stains, has become common practice in recent years [1, 2]. Laser light of an appropriate wavelength (585 nm) is used because it is highly absorbed by the target chromophore, hemoglobin, within the vasculature. This absorption of energy induces the desired thermal necrosis of the hypervascular lesions. However, melanin within the epidermis also absorbs a wide spectrum of light energy. To avoid epidermal injury by heating, a method of precooling using a short duration refrigerant spray has found widespread acceptance because of the possible high heat fluxes and precise control of cooling duration [3]. Thus, rapid and spatially selective cooling of the epidermis is possible without lowering the temperature of the deeper-seated target chromophores. With precooling, the epidermis is kept below the damage threshold during heating of the tissue by the subsequent laser pulse.

Despite the effectiveness of this epidermal protection technique, complete blanching of the lesions is rarely achieved. Darker-skinned patients also normally cannot be treated. Treatment effectiveness could potentially be improved by increasing laser fluence, but this is limited by the epidermal protection that the sprays can provide. Additionally, the sprays have been found to induce highly non-uniform cooling [4], potentially leading to uneven protection and skin dyspigmentation or scarring. Many studies have been done to characterize these refrigerant sprays and their accompanying heat transfer [5-8], but the mechanisms of atomization and heat transfer are still not well understood.

Recently, a new treatment technique using vacuum suction cups to dilate the blood vessels and increase blood volume fraction prior to laser treatment has shown promising results [9, 10]. Improved blanching with the same radiant exposure is possible. As air is evacuated from these suction cups, both air pressure and humidity are reduced. In general, humidity can also vary in the environment without the use of the suction cups. The effects of hypobaric pressures and changing humidity on the spray itself have not been quantitatively identified. Therefore, the purpose of this study is to quantitatively characterize the spray and observe the changes due to varying ambient pressure and humidity. Explanations for the observed changes will be given, along with implications on heat transfer.

## Experimental Methods

### *Spray system*

The liquid refrigerant used was R-134a (1,1,1,2-tetrafluoroethane; National Refrigerants, Philadelphia, PA) which was maintained at saturation pressure 660 kPa at room temperature) in a standard 30 lb bottle.

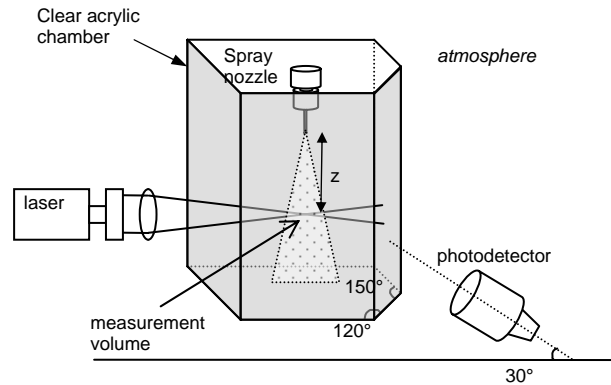


**Figure 1.** A schematic of the PDPA system and clear acrylic chamber.

The refrigerant was delivered via a high pressure hose to a clinically-used solenoid valve and nozzle (GentleLASE™; Candela, Wayland, MA). The nozzle was a stainless steel plain circular orifice tube of 0.5 mm inner diameter and approximately 25 mm length. There was a 20° bend in the nozzle near the solenoid valve body, but the nozzle exit was oriented to deliver horizontal sprays. Axial positions,  $z$ , were defined as the vertical distances between the nozzle exit tip and the probe measurement volume. The solenoid valve and nozzle were displaced using a commercial translational axis (Pittman Lo-Cog, Harveysville, PA) to desired  $z$  spanning 15 to 90 mm with 15 mm increments. Errors in  $z$  were approximately  $\pm 1$  mm. In clinical practice,  $z$  is normally fixed at 30 mm so this study includes the clinically relevant distance.

### *Spray characterization*

Spray droplet velocity and diameter were measured using a Phase Doppler Particle Analyzer (PDPA; TSI Incorporated, Shoreview, MN) with an Argon ion laser emitting 488 and 514.5 nm wavelength light beams. A schematic of this setup is shown in Figure 1. This system was capable of measuring velocity along two perpendicular axes, but only the axial velocities will be presented since the magnitudes of the lateral (radial) velocities were significantly smaller. All presented PDPA diameter and velocity values were averages of a minimum of 10000 measurement points taken from steady-state sprays. According to Tate and Marshall [11], this corresponds to an error in cumulative distribution of less than 1.5%.  $D_{10}$  averaging of diameter was used because it is a first-order expression and, therefore, less sensitive to measurement errors.

### *Ambient condition control*

In order to control the ambient pressure and humidity of the environment surrounding the nozzle, a custom

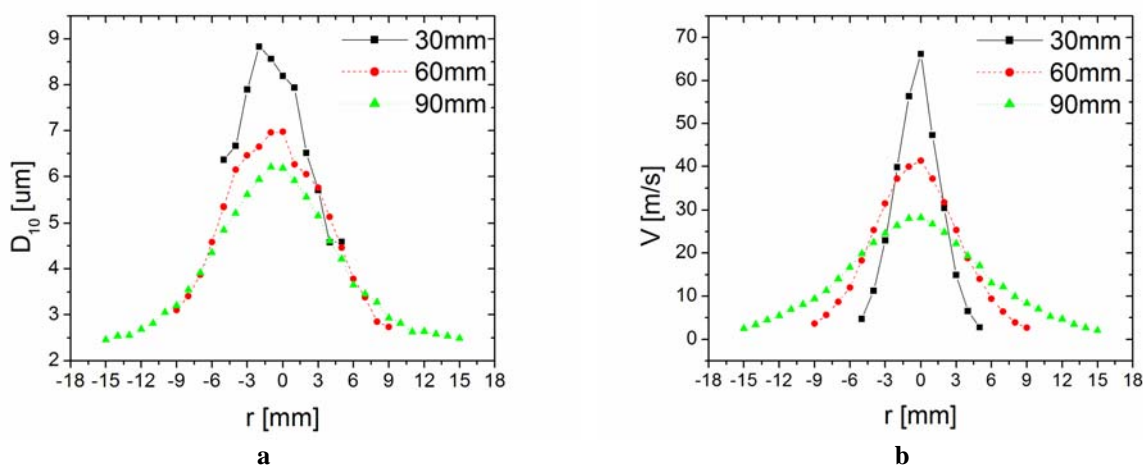


**Figure 2.** a)  $D_{10}$  and b) velocity cross-sectional measurements of the spray at atmospheric pressure.

clear acrylic chamber was designed and fabricated to enclose the spray system. The chamber walls were 12.7 mm thick to withstand the vacuum pressures needed for the study. The walls were also designed to be perpendicular to the paths of incident and scattered light to minimize refraction. The walls were found to slightly decrease diameter measurements (1–2 μm) while having no perceivable influence on velocity measurements. The changes in diameter were considered to be a systematic error so relative comparisons of measurements with the chamber in place could still be made. Gauge pressures for the study were 0, -17, -35, and -50 kPa. Vacuum pressures were obtained using the building vacuum system. Relative humidities of 15, 35, 55, and 75% were obtained by either introducing saturated air into the chamber using an ultrasonic humidifier (Kaz Inc., Hudson, NY) or flushing with dry air.

#### *Spray imaging*

Still images of the spray were taken using a high speed camera (Photron Fastcam; San Diego, CA) with a 1/30 s frame rate and 1/60 s shutter speed. Lighting was provided by a standard 75 W incandescent light bulb positioned slightly to the right and above the spray system to prevent glare from reflections with the acrylic chamber walls.

#### **Results**

Steady-state measurements taken without the clear acrylic chamber are shown in Figure 2 for axial locations of  $z=30$ , 60, and 90 mm across the entire spray area. For these measurements, temperature was maintained at 24 °C with approximately 35 % relative humidity at atmospheric pressure.  $D_{10}$  and velocity measurements show symmetric bell-shaped distributions of drop sizes, except at  $z = 30$  mm.

Humidity tests using the clear acrylic chamber showed visible changes in the spray. Figure 3 shows still images taken of the steady-state spray at 15% and 75% relative humidities. Visually, the increased humidity appears to increase spray penetration (axial distance of spray extension from nozzle tip) and spray cone diameter significantly. The length of penetration could not be determined because the spray reached the bottom of the chamber which was approximately 40 cm from the nozzle tip. It is important to note that images of the spray change drastically depending on the lighting used. For this study, the spray may not have been fully illuminated so spray cone diameters and penetration may actually be greater than they appear. PDPA measurements along the spray cross-section at  $z=30$ mm and at the center of the spray at  $z=90$ mm did not indicate a detectable change in spray droplet characteristics through this range of humidities so they are not presented.

Contrary to humidity changes, reductions in ambient pressure resulted in changes in the spray characteristics. Generally, with decreasing pressure there is a simultaneous decrease in droplet size and increase in velocity as indicated in Figure 4. The rate of change of diameter and velocity, as indicated by the slopes of the lines of Figure 4 a and b, remains fairly constant as ambient pressure is reduced. For  $z = 15$  mm, the measurements are within a very dense portion of the spray so they are more prone to errors. The fact that  $D_{10}$  for  $z = 15$  and 30 mm nearly coincide may be in part due to measurement error. Figures 4c and d show the same data plotted as a function of  $z$ . Notice the wavy nature of the diameter plots in Figure 4c which gradually dampens as pressure is reduced. Figure 4d shows a much smoother transition from high to low velocity with increasing  $z$ . With

reducing pressure, the curves are simply shifted upward with little change in slopes.

Lastly, Weber numbers, defined generally as  $(\rho u^2 d_{\text{droplet}})/\sigma$ , were calculated from the above PDPA measurements. Two forms of Weber number are actually in use, and they provide information about different aspects of the spray. Their difference lies in what medium is used for density, the fluid composing the droplet (R134a) or the surrounding dispersed fluid (air/vapor).

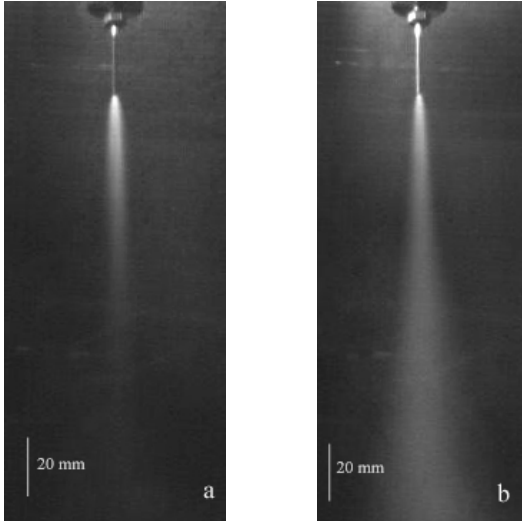


**Figure 3.** Still images of the spray with a) 20% relative humidity and b) 75% relative humidity.

The former, denoted  $We_d$  in this study, provides the ratio of droplet inertial forces to droplet surface tension forces and is typically used in heat transfer studies [7, 12-14]. The latter,  $We_a$ , is the ratio of aerodynamic forces to droplet surface tension and is a measure of droplet stability or likelihood of breaking up in flight due to drag forces with the surround medium [15-17]. Droplets are generally assumed to be stable below critical values of between 10-20 [16]. The density and surface tension of R134a were assumed to be constant values of  $1234 \text{ kg/m}^3$  and  $0.0079 \text{ N/m}$ , respectively. The density of the surrounding medium was assumed to be that of pure air, and a function of the absolute pressure within the chamber. Calculations of  $We_d$  are provided in Figure 5 and indicate a slight increase with decreasing pressure.  $We_a$  values were also calculated and all were found to be below critical, ranging from 5.5 to 0.5. For brevity, these values are not presented.

### Discussion

The diameter profile of Figure 2a indicates that the spray is generally better atomized near the cone edge so the nozzle walls may be contributing to the atomization process during or immediately proceed-

ing internal flow. The slight asymmetry in diameter with radial location is possibly due to the influence of valve or nozzle irregularities in interior surface roughness or the shape of the orifice. This asymmetry in diameter profile appears to be dampened at further locations. For velocity, the radial symmetry is more apparent and at  $z=30\text{mm}$ , it steeply decreases from  $67 \text{ m/s}$  to nearly  $0 \text{ m/s}$ . This profile may, again, stem from the velocity profile of internal flow within the nozzle. Relaxation of both profiles, due to interaction with the surrounding air, occurs as the droplets travel further away from the nozzle tip, and is accompanied by an increase in the overall spray area. The cross-sectional non-uniformity of spray droplet diameter and velocity may arise because of the simplicity of the plain orifice atomization device. These profiles are a function of the device used, but for some other full-cone sprays, velocity and diameter profiles are often assumed to be uniform and only a function of  $z$  [12, 18].

Though humidity changes did not appear to influence droplet spray characteristics, the visible increase in spray cone diameter and penetration may be an indication of water condensation from the air. Following spray termination at 55% and 75% relative humidity, a haze circulated in the chamber and persisted for some time. This haze did not exist for lower humidities so it may be evidence of small water droplets. In a previous work [19], surface ice was thought to form only after spray termination and recession of the liquid film layer on a flat rigid substrate because of the refrigerant's hydrophobic nature. The images of Figure 3 suggest that this may not be the case because water droplets may condense in flight during the spray duration. This would explain the step-like decrease in temperature that is occasionally observed in heat transfer measurements due to periodic formation and sloughing of an insulating ice layer on the surface of the substrate [19].

The diameter measurements of the at atmospheric pressures show some differences from previous work [20].  $D_{32}$  measurements using an Ensemble Particle Concentration and Sizing apparatus (EPCS; Insittec/Malvern, Worcestershire, UK) showed diameters ranging from  $2\text{--}5 \mu\text{m}$  for  $z = 10\text{--}160 \text{ mm}$  for the same valve and nozzle used in this study. Sizes were actually found to increase slightly between  $z = 10\text{--}60 \text{ mm}$  before decreasing again. This was attributed to possible droplet coalescence in flight. Figure 4c, however, shows a continuous decrease in diameter with increasing  $z$ . The difference may arise because the EPCS system measures an average of all droplet sizes crossing a laser beam of  $3 \text{ mm}$  diameter whereas the PDPA system measures a much smaller area of approximately  $60 \times 600 \mu\text{m}$ . Because of the non-uniformity in the spray cross-section, PDPA

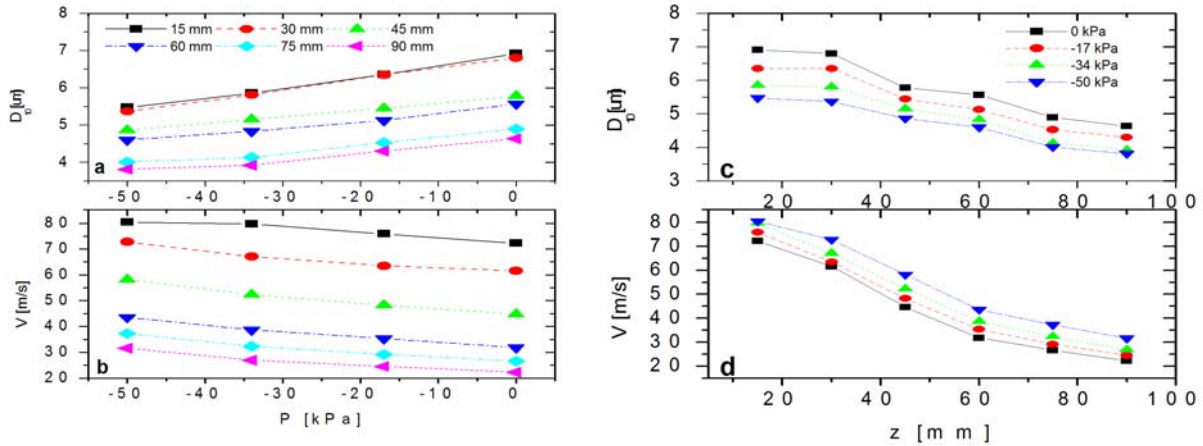


**Figure 4.** PDPA measurements of **a)**  $D_{10}$  and **b)** axial velocity with respect to  $P$  and the same measurements of **c)**  $D_{10}$  and **d)** axial velocity with respect to  $z$ .

point measurements are more capable of resolving the spray droplet distribution and change with  $z$ . These new measurements show that droplet coalescence may not be a significant factor and that droplets will generally decrease in size with increasing  $z$ . The magnitudes of the droplet sizes for the two techniques are similar, but PDPA results show slightly larger droplets. These differences are, again, attributed to the differences in average droplet representation ( $D_{10}$  vs.  $D_{32}$ ), measuring techniques and calibrations.

The velocity measurements at ambient conditions again show some differences with Aguilar et al. [20] in which a time of flight technique was used. This technique was not capable of resolving the changes in velocity that the PDPA measurements show. Velocity gradient is high at first and then decreases for larger  $z$  as shown in Figure 4d. This is due to the fact that as velocity decreases, the corresponding drag force on the droplet also decreases. Acceleration, likewise, will decrease.

Although there is no conclusive proof of the origin of the slightly wavy nature of the diameter variation with axial location seen in Figure 4c, we speculate this is due to changes in the local surrounding refrigerant vapor concentrations. At the nozzle exit, a two-phase vapor-liquid effluent exists. The high concentration of vapor likely inhibits the evaporation of the droplets, so droplet sizes remain steady at distances near to the nozzle exit. Between  $z = 30$  and 45 mm, sufficient vapor has diffused away from the liquid-air interface and droplet evaporation increases. This is followed by another region of high vapor concentration and slowed droplet evaporation and the cycle repeats itself. As ambient pressure is decreased, this oscillating phenomenon is dampened, as indicated by the smoothing of the lines. The decrease in

air density reduces the resistance to vapor diffusion so droplet evaporation may occur at a more consistent rate.

The changes in spray diameter and velocity due to vacuum pressures may be due to two effects: the increase in pressure differential across the spray nozzle, and the reduction of ambient air density. The increase in pressure differential has the effect of increasing effluent velocity and promoting primary atomization. The reduction in air density promotes droplet evaporation due to less resistance to refrigerant vapor diffusion from the liquid-gas interface while also reducing the drag forces on the droplets in flight. Based on the data presented, it appears that the former is the more dominant mode of influence because most of the changes are apparent at  $z=15$  mm (close to the nozzle exit) and persist as  $z$  increase, *i.e.*, the slopes of the lines of Figure 4ab are similar. Therefore, most of the changes due to the pressure changes on the spray likely occur either within the nozzle or shortly after exiting the nozzle. This suggests that the primary mode of influence of reducing ambient pressures is the increase in pressure drop through the nozzle while air density reductions are of secondary importance.

Calculated  $We_a$  numbers are well below the established critical value of between 10 to 20 [16] so the spray appears to be well atomized, consisting of small spherical droplets. The change in droplet sizes beyond  $z = 15$  mm, again, is likely only due to droplet evaporation, not secondary atomization from shearing forces with the surrounding air. Because of the density of the spray before 15mm, measurements may not be reliable so spray characteristics would be difficult to characterize with the PDPA. Nonetheless, the fine atomization of the spray resulting from a simple plain-orifice nozzle would suggest that the

spray atomization is dominantly a function of thermodynamic mechanisms, not hydrodynamic as is the case for most other cooling sprays. The thermodynamic instability of the refrigerant due to the sudden and large pressure drop may induce a flash boiling event within the nozzle and/or immediately at the nozzle exit [21]. This violent expansion of the fluid causes it to break up immediately into fine droplets. Further studies are, of course, needed to confirm these theories..

The measured changes in  $We_d$  spray characteristics may have important implications for heat transfer. It is well known that heat flux from sprays can be correlated with  $We_d$  [12, 13] and this, in fact, has been done for dermatological cooling studies [7]. Higher  $We_d$  droplets are more capable of penetrating the liquid film that forms at the surface of the cooling surface and can thereby increase the intensity of heat extraction. The present study shows a slight increase in  $We_d$  for most  $z$  as pressure is reduced, but Aguilar *et al* [9] found that with concurrent decrease in ambient pressures and humidity, the maximum obtainable heat fluxes of R134a sprays were reduced [9].

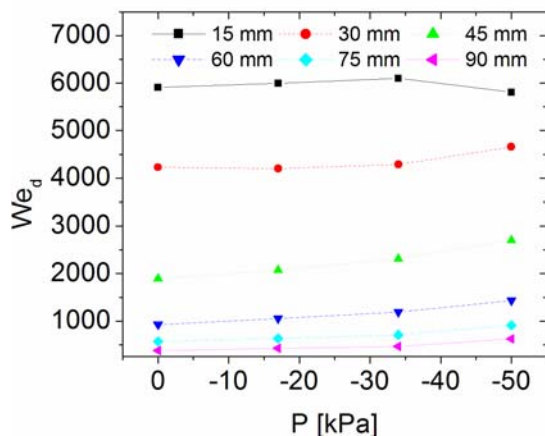


Figure 5. Calculations of  $We_d$  with respect to  $z$ .

This contradictory result may indicate that the reduction of pressure introduces other mechanisms that influence heat flux besides  $We_d$ .

### Conclusions

- Measurements of the spray at atmospheric conditions show highly non-uniform distributions of droplet diameter and velocity along the spray cross-section.
- While humidity does not affect droplet diameter and velocity within the measured locations, spray cone radius and penetration are visibly increased.

- Reductions in ambient pressure serve to reduce droplet size by  $\sim 0.5 \mu\text{m}$  while simultaneously increasing droplet velocity by  $\sim 10 \text{ m/s}$  for all  $z$ .
- $We_d$  values range from 5.5 to 0.5 and indicate hydrodynamically stable droplets through a range of  $z$  of 15-90 mm. The simple plain-orifice device used in this study is capable of producing a finely atomized spray.
- $We_d$  are mainly a function of  $z$  varying from 200 to 6000 though they may increase slightly as pressure is reduced.
- Based on established correlations between spray  $We_d$  and heat flux, the slight increase in  $We_d$  with decreasing pressures does not agree with previous heat transfer studies that show a decrease in heat flux. The pressure effects on the heat transfer mechanisms for this particular application needs to be studied further.

### Acknowledgements

The authors would like to acknowledge the frequent useful discussions with Jie Liu and laboratory assistance provided by Kevin Chu and Will Macias.

### References

1. Nelson J., Milner TE, Anvari B, Tanenbaum BS, Kimel S, Svaasand LO, Jacques SL, *Dynamic epidermal cooling during pulsed laser treatment of port wine stain. A new methodology with preliminary clinical evaluation.* Arch. Dermatol., 1995. **131**: p. 695-700.
2. Torres JH, Nelson JS, Tanenbaum BS, Milner TE, et al., *Estimation of internal skin temperatures in response to cryogen spray cooling: Implications for laser therapy of port wine stains.* IEEE J. Selected Topics Quantum Electron., 1999. **5**: p. 1058-1066.
3. Verkruysee W, Majaron B, Tanenbaum BS, Nelson JS, *Optimal cryogen spray cooling parameters for pulsed laser treatment of port wine stains.* Lasers Surg Med, 2000. **27**: p. 165-170.
4. Franco W, Liu J, Wang GX, Nelson JS, Aguilar G, *Radial and temporal variations in surface heat transfer during cryogen spray cooling.* Phys Med Biol, 2005. **50**: p. 387-397.
5. Aguilar G, Majaron B, Verkruysee W, Zhou Y, Nelson JS, Lavernia EJ, *Theoretical and experimental analysis of droplet diameter, temperature, and evaporation rate evolution in cryogenic sprays.* Int J Heat Mass Transfer, 2001. **44**: p. 3201-3211.
6. Aguilar G, Majaron B, Verkruysee W, Nelson JS, Lavernia EJ, *Characterization of*

- cryogenic spray nozzles with application to skin cooling.* in *Proceedings of IMECE 2000: The International Mechanical Engineering Congress and Exposition*. 2000. Orlando, Florida: ASME.
7. Pikkula BM, Tunnell J, Anvari B, *Methodology for characterizing heat removal mechanism in human skin during cryogen spray cooling.* *Annals of Biomedical Engineering*, 2004. **31**: p. 493-504.
  8. Pikkula BM, Tunnell J, Chang DW, Anvari B, *Effects of droplet velocity, diameter, and film height on removal during cryogen spray cooling.* *Annals of Biomedical Engineering*, 2004. **32**(8): p. 1131-1140.
  9. Aguilar G, Franco W, Liu J, Svaasand L, *Effects of hypobaric pressure on human skin: Implications for cryogen spray cooling (Part II).* *Lasers Surg Med*, 2005. **36**: p. 130-135.
  10. Aguilar G, Svaasand L, Nelson JS, *Effects of Hypobaric Pressure on Human Skin: Feasibility Study for Port Wine Stain Laser Therapy (Part I).* *Lasers Surg Med*, 2005. **36**: p. 124-129.
  11. Tate RW, Marshall WR, *Atomization by centrifugal pressure nozzles.* *Chemical Engineering Progress*, 1953. **49**(4): p. 169-174.
  12. Hsieh SS, Fan TC, Tsai HH, *Spray cooling characteristics of water and R-134a. Part I: nucleate boiling.* *Int J Heat Mass Transfer*, 2004. **47**: p. 5703-5712.
  13. Hsieh SS, Fan TC, Tsai HH, *Spray cooling characteristics of water and R-134a. Part II: transient cooling.* *Int J Heat Mass Transfer*, 2004. **47**: p. 5713-5724.
  14. Incropera FP, DeWitt DP, *Fundamentals of Heat and Mass Transfer*. 4th ed. 1996, New York: John Wiley and Sons. 885.
  15. Hinze J, *Fundamentals of the hydrodynamic mechanism of splitting in dispersion processes.* *AIChE*, 1955. **1**: p. 289-295.
  16. Lefebvre A, *Atomization and Sprays*. Combustion, 1040-2756. 1989, New York: Hemisphere Pub. Corp. 421.
  17. Ranger A, Nicholls J, *Use of breakup time data and velocity history data to predict the maximum size of stable fragments for acceleration-induced breakup of a liquid drop.* *Int J Multiphase Flow*, 1969. **13**: p. 741-757.
  18. Ghodebane M., Holman JP, *Experimental study of spray cooling with Freon-113.* *Int J Heat Mass Transfer*, 1991. **34**(4/5): p. 1163-1174.
  19. Majaron B, Kimel S, Verkruysee W, Aguilar G, Pope K, Svaasand LO, Lavernia EJ, Nelson JS, *Cryogen spray cooling in laser dermatology: Effects of ambient humidity and frost formation.* *Lasers Surg Med*, 2001. **28**: p. 469-476.
  20. Aguilar G, Majaron B, Karapetian E, Lavernia EJ, Nelson JS, *Experimental study of cryogen spray properties for application in dermatological laser surgery.* *IEEE Transactions on Biomedical Engineering*, 2003. **50**(7): p. 863-869.
  21. Reitz RD, *A photographic study of flash-boiling atomization.* *Aerosol Science and Technology*, 1990. **12**: p. 561-569.

